Transport properties of Ru-doped $La_{1.85}Sr_{0.15}CuO_4$ and the effect of carrier concentration compensation

2003 J. Phys.: Condens. Matter 15 1693

(http://iopscience.iop.org/0953-8984/15/10/317)

INSTITUTE OF PHYSICS PUBLISHING JOURNAL OF PHYSICS: CONDENSED MATTER

J. Phys.: Condens. Matter **15** (2003) 1693–1704 PII: S0953-8984(03)37638-6

Transport properties of Ru-doped $La_{1.85}Sr_{0.15}CuO_4$ and the effect of carrier concentration compensation

Y M Xiong, L Li, X G Luo, H T Zhang, C H Wang, S Y Li and X H Chen[1]

Structure Research Laboratory and Department of Physics, University of Science and Technology of China, Hefei, Anhui 230026, People's Republic of China

E-mail: chenxh@ustc.edu.cn

Received 31 May 2002
Published 3 March 2003
Online at stacks.iop.org/JPhysCM/15/1693

Abstract

This paper is a study of the structure and transport properties of Ru-doped $La_{1.85}Sr_{0.15}CuO_4$. It is found that Ru substitution for Cu has two effects. (1) Ru doping introduces disorder into the system, which causes a metal–insulator transition with high localization. (2) There is a hole-filling effect due to the valence of the Ru ion being higher than that of the Cu ion. Increase of the strontium content could compensate for the imbalance of valence caused by doping with the high-valence Ru ion. A universal curve for T_c versus the number of holes per Cu site is observed for the $La_{2-y}Sr_yCu_{1-x}Ru_xO_4$ system, indicating that a rigid-band model holds and T_c correlates with features in the density of states, such as a Van Hove singularity.

1. Introduction

The discovery of superconductivity in doped La_2CuO_4 (La214) by Bednorz and Müller [1] has stimulated an enormous number of studies of these lamellar copper oxide materials. In order to improve our understanding of high-temperature superconductivity, a careful study of transport and the unusual normal-state (NS) properties of high-temperature superconductors is required. Element doping at the Cu sites and non-Cu sites offers an important route towards this goal. Much work has been done on substituting a great variety of metals for copper in $La_{1.85}Sr_{0.15}CuO_4$ (LSCO) [2–14]. According to previous studies, the superconducting transition temperature (T_c) is found to depend on the crystallographic structure, carrier concentration, and substitutional impurities on the Cu sites of these compounds. As we know, conventional superconductors are very sensitive to magnetic element doping, while cuprate superconductors seem not so sensitive to magnetic element doping at non-Cu sites as conventional superconductors. For the substitution of elements for Cu in Cu–O sheets, both

[1] Author to whom any correspondence should be addressed.

magnetic ion and non-magnetic ion doping can destroy the superconductivity with just a small percentage dopant concentration. The La214 system is an ideal system in which to study the effect of chemical substitution on superconductivity and NS properties, because studying this system avoids concerns regarding any contribution to NS properties from charge reservoirs in the non-superconductive intergrowth layers.

The superconductivity of hole-type cuprates had been confirmed to be of a d-wave type [15], and antiferromagnetic interaction within the CuO_2 plane has received more attention than ever as a candidate origin for the superconductivity [16, 17]. Xiao *et al* [18] had demonstrated that the suppression of superconductivity by elemental doping originated from a magnetic pair-breaking effect. It was reported by Maeno *et al* that Sr_2RuO_4 becomes superconducting at a very low temperature ($T_c = 0.93$ K) [19]. Recently much work had been done on Sr_2RuO_4 [20–24]. Both $La_{2-y}Sr_yCuO_4$ and Sr_2RuO_4 adopt the K_2NiF_4-type structure. However, the superconductivity of Sr_2RuO_4 was proved to be p-wave symmetrical and induced by ferromagnetic spin fluctuations [25–27]. Additionally, Ru^{4+} (like Ru^{5+}) is a typical magnetic ion and it also shows great solubility in the La214 system [28]. So we focused our attention on the system $La_{2-y}Sr_yCu_{1-x}Ru_xO_4$, which may be considered as a combination of these two known superconductors. Recent x-ray absorption near-edge-structure (XANES) measurements revealed formal oxidation states between +4 and +5, instead of +6, for the ruthenium ions, whereas the oxidation state of the Cu ions remained +2 [14]. The doping with high-valence ruthenium ions causes imbalance of the valence in this system. We synthesized double-doped samples of $La_{2-y}Sr_yCu_{1-x}Ru_xO_4$. In these samples, Ru ions directly replace Cu sites on the CuO_2 plane, inducing extra electrons in the conducting layer [11]. We increased the content of Sr^{2+} ions substituting for La^{3+} to provide carriers of holes, and studied the effect of carrier concentration on superconductivity in this way.

2. Experimental details

Samples of $La_{2-y}Sr_yCu_{1-x}Ru_xO_4$ were prepared by conventional solid-state reaction. Appropriate amounts of La_2O_3, $SrCO_3$, CuO, and RuO_2 were ground in an agate mortar. The mixtures were reacted in alumina crucibles at 850 °C for 24 h. The loose mixture powder was reground and pressed into pellets. After that these pellets were sintered at 1150 °C for 48 h with one intermediate grinding and pelletizing.

Powder x-ray diffraction (XRD) measurements were carried out with a Rigaku D/max-γA x-ray diffractometer with graphite-monochromatized Cu Kα radiation ($\lambda = 1.5406$ Å). Resistivity measurements were performed by the standard four-probe method in the temperature range from room temperature down to 4.2 K. The lattice parameters were established by the Rietveld method using GSAS.

3. Results and discussion

Figures 1 and 2 show the XRD patterns for the samples of $La_{1.85}Sr_{0.15}Cu_{1-x}Ru_xO_4$ with $x = 0$, 0.01, 0.03, 0.05, and 0.1, and of $La_{1.85-2x}Sr_{0.15+2x}Cu_{1-x}Ru_xO_4$ with $x = 0$ and 0.1. All powder XRD patterns shown in figures 1 and 2 indicate that all samples were single phase. They can be indexed with a tetragonal lattice. The lattice parameters were obtained by fitting the data from the XRD patterns using the Rietveld method. Figure 3 shows the variation of the lattice parameters a, c and the ratio c/a with x for the samples of $La_{1.85}Sr_{0.15}Cu_{1-x}Ru_xO_4$ and $La_{1.85-2x}Sr_{0.15+2x}Cu_{1-x}Ru_xO_4$. It is apparent that the lattice parameter a increases continuously with increase of x, while the parameter c and the ratio

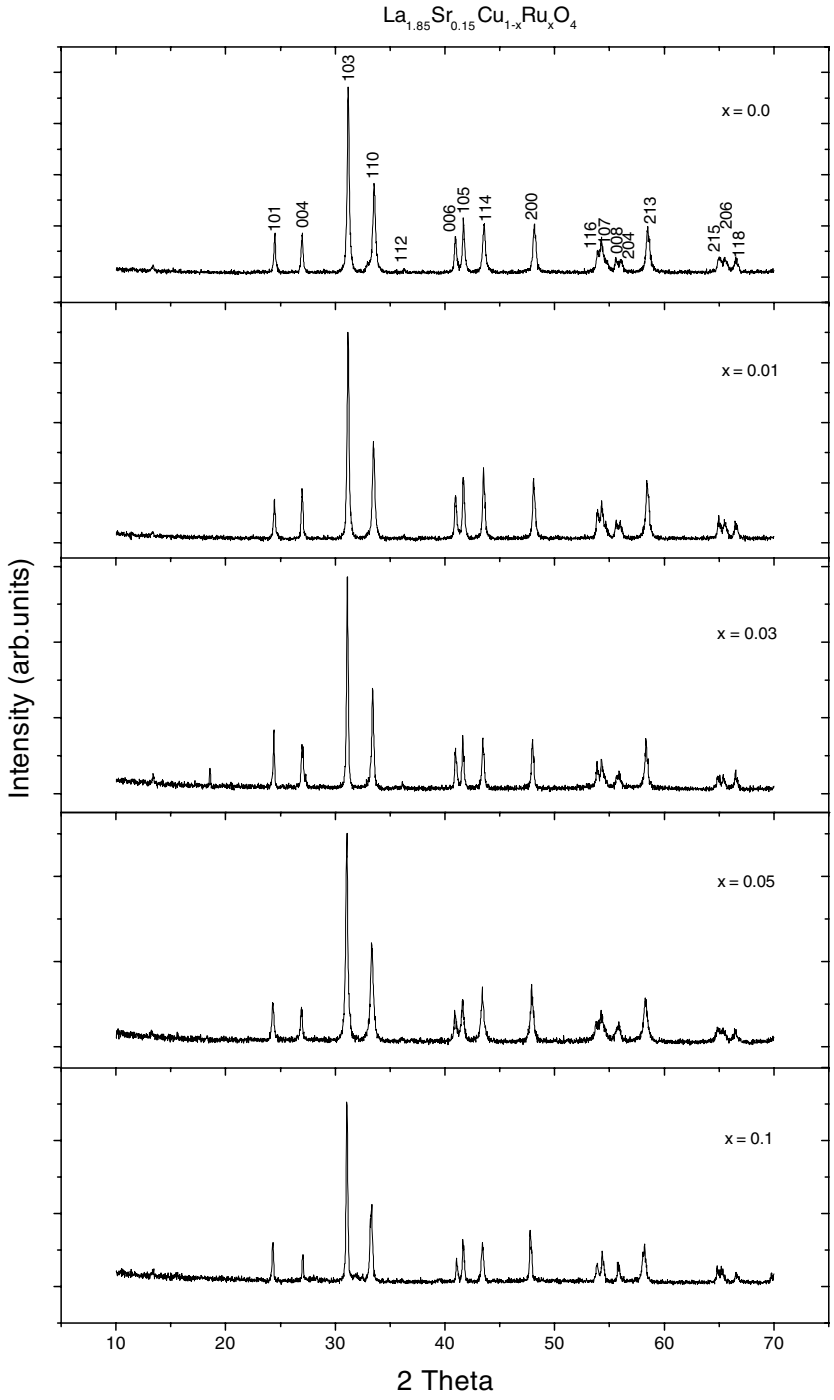

Figure 1. Typical XRD patterns of samples of $La_{1.85}Sr_{0.15}Cu_{1-x}Ru_xO_4$ ($x = 0$, 0.01, 0.03, 0.05, 0.1).

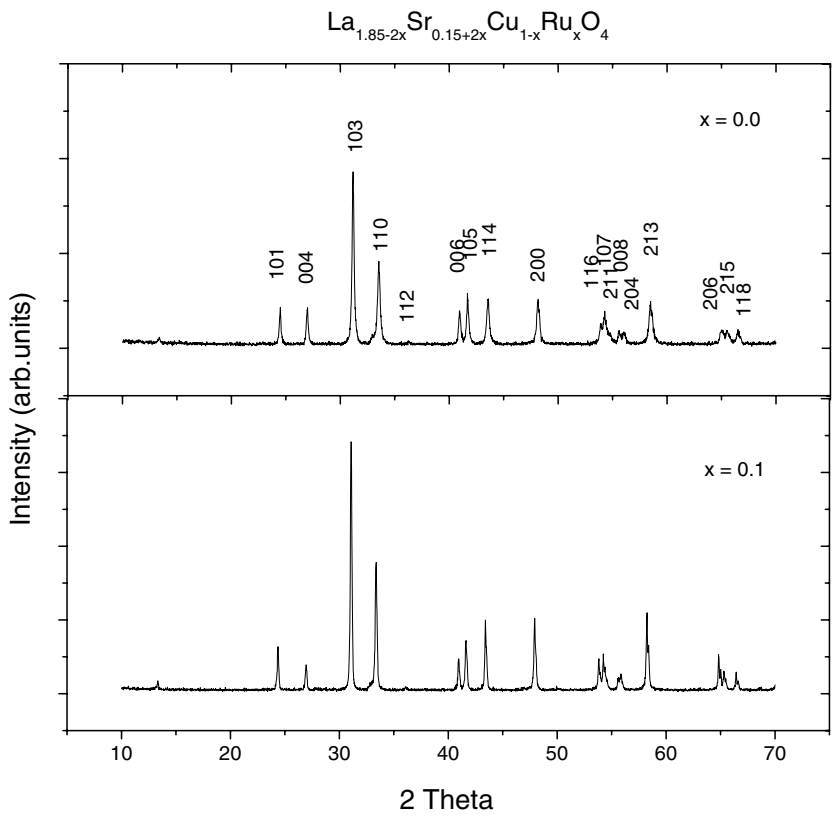

Figure 2. Typical XRD patterns of samples of $La_{1.85-2x}Sr_{0.15+2x}Cu_{1-x}Ru_xO_4$ ($x = 0, 0.1$).

c/a monotonically decrease with x. The change of the lattice parameters for the samples $La_{1.85}Sr_{0.15}Cu_{1-x}Ru_xO_4$ with increase of the ruthenium content x should arise from four aspects, mainly. The first one is the different electronic states of the Ru^{4+} and Cu^{2+}. We know that Ru^{4+} is a $4d^4$ system, which possesses a low-spin $^3T_{1g}$ ground state in an octahedral oxygen coordination, from magnetic measurements. The resulting Jahn–Teller activity is strongly reduced by spin–orbit coupling which leads to a non-degenerate ground state ($J = 0$) [29]. On the other hand, Cu^{2+}, as a $3d^9$ system (^2E_g ground state), shows a strong Jahn–Teller effect. So the change of parameters should partly arise from the contribution from the replacement of an ion with high Jahn–Teller activity by an ion with low Jahn–Teller activity. The ratio c/a is used to characterize the Jahn–Teller distortion of the CuO_6 octahedra. In such conditions, the Cu/Ru–O octahedron was reduced along the c-axis and elongated along the a-axis. Therefore, the ratio c/a decreases. The second aspect is, directly, the different ions radii of Ru^{4+} and Cu^{2+}. The radius of Ru^{4+} with sixfold oxygen coordination is 0.76 Å, which is smaller than 0.91 Å, the radius of Cu^{2+} [30]. This induces decreases of the parameters a and c. The third aspect is the different Madelung potentials of Ru and Cu ions. Their Madelung energy can be given by the following formula [31]:

$$\mu_M = -\frac{N\alpha Z_+ Z_- e^2}{4\pi\varepsilon_0 R_0} \tag{1}$$

where N is the number of positive and negative ion pairs, Z_+ and Z_- is the charge of positive or negative ions respectively, α is the Madelung constant and relates to the structure of the

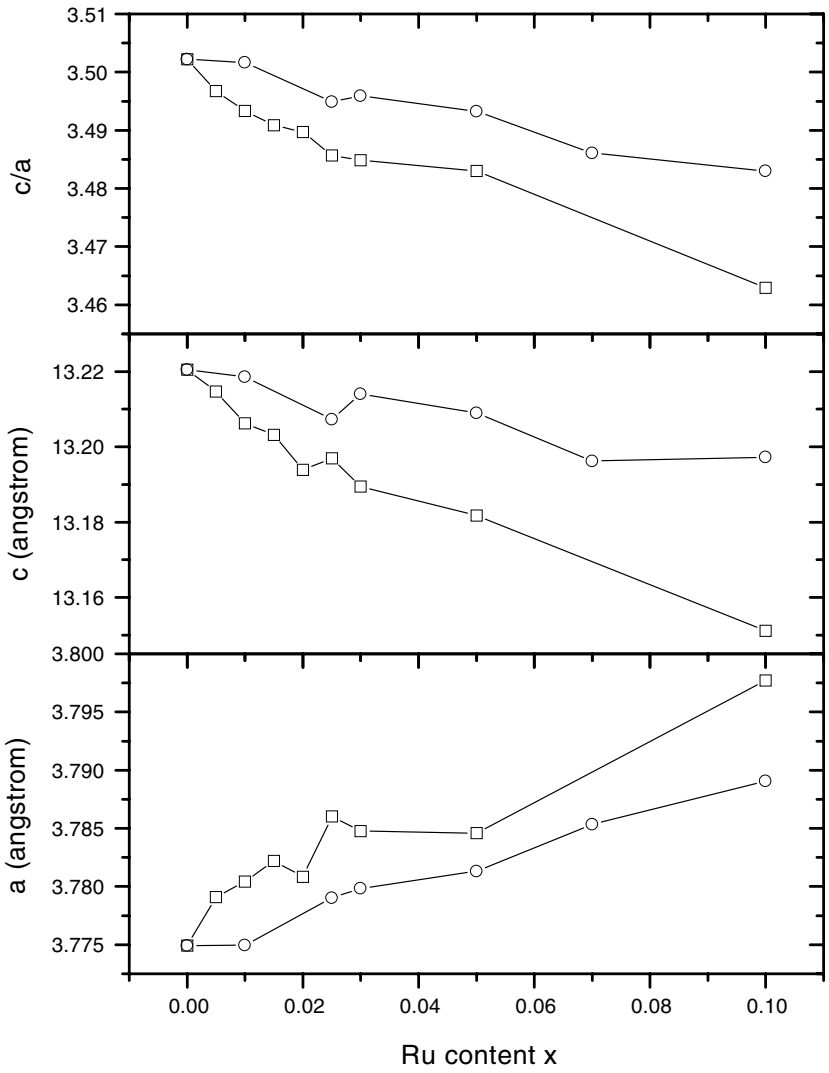

Figure 3. The lattice parameters a and c and the ratio of c/a as a function of Ru content x for $La_{1.85}Sr_{0.15}Cu_{1-x}Ru_xO_4$ (□) and $La_{1.85-2x}Sr_{0.15+2x}Cu_{1-x}Ru_xO_4$ ($0 \leqslant x \leqslant 0.1$) (○).

lattice. The minus sign in front of the formula indicates that the Madelung energy is a kind of attraction energy. The Ru ions are expected to attract the neighbouring oxygens ions, causing a contraction of the CuO_6 octahedron. Since the apical O(2)s are much more weakly bound than the O(1)s in the Cu–O plane, the effect of contraction on O(2) will be much stronger. It leads to a decrease in the parameter c (and in c/a) much larger that than in the parameter a. The last aspect is the addition of electrons into antibonding orbitals caused by Ru doping. This causes the in-plane Cu–O bond to expand [32, 33], as observed. As can be seen from the above discussion, the decrease of the parameter c (and c/a) and the increase in a are cooperative effects with four causes. Decrease in Jahn–Teller activity and the expansion of in-plane Cu–O bonds due to the addition of electrons into antibonding orbitals caused by Ru doping leads to an increase in parameter a, whereas the decrease of the ion radius and stronger Madelung

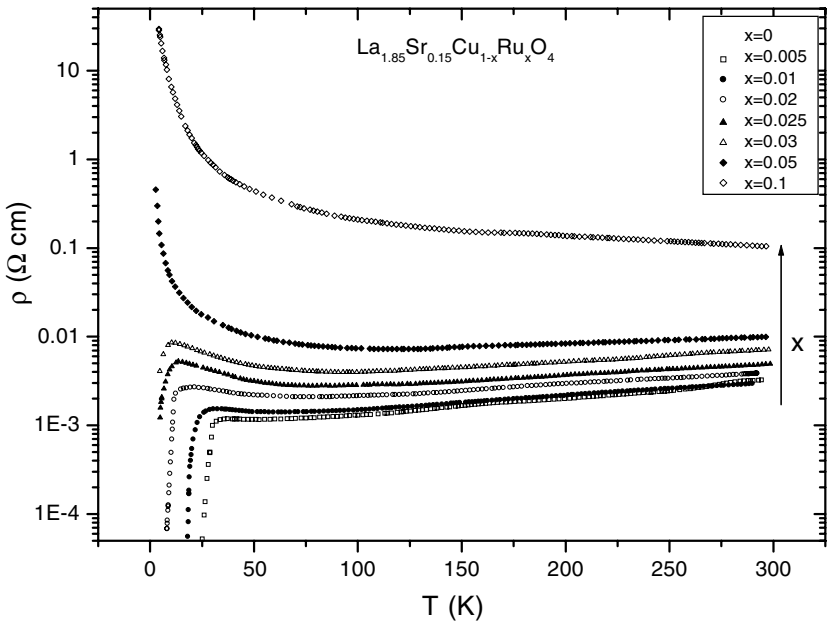

Figure 4. The temperature dependence of the resistivity for samples of $La_{1.85}Sr_{0.15}Cu_{1-x}Ru_xO_4$ ($x = 0$, 0.005, 0.01, 0.02, 0.025, 0.03, 0.05, 0.1).

potentials of Ru ions cause it to decrease. Because the effect of the former is larger than that of the latter, the total effect of Ru doping makes the parameter a increase. The change of lattice parameters provides evidence that Cu ions were replaced by Ru ions. On the other hand, for the Ru214 phase, it is most likely that Ru ions were substituted for Cu.

As can be seen in figure 3, the parameter a decreases with increase in strontium content at the same ruthenium content, and the parameter c increases. With increase of the strontium content, the hole carrier concentration in CuO_2 planes increases, which leads to a significant reduction of the Cu–O(1) bond length [32, 33]. This causes decrease of the parameter a. The parameter c is mainly affected by the strontium ion radius. The radius of Sr^{2+} is 1.40 Å, which is larger than 1.30 Å, the radius of La^{3+} [30]. As discussed above, the difference in Madelung potentials of Sr^{2+} and La^{3+} also contributes to the c-axis expansion in the LSCO system; while hole doping via Sr substitution for La into $x^2 - y^2$ orbitals causes enhancement of the Jahn–Teller distortion of the CuO_6 octahedra. These effects lead to a decrease in a and an increase in c.

Figure 4 shows the temperature dependence of the resistivity for $La_{1.85}Sr_{0.15}Cu_{1-x}Ru_xO_4$ between 4.2 and 300 K. With increase of the ruthenium content, T_c is suppressed rapidly. For $x = 0.025$, the zero resistivity is not obtained at temperatures down to 4.2 K. With further increasing ruthenium content, the upturn of the resistivity at low temperature becomes more obvious, indicating a localization effect due to doped ruthenium ions on the two-dimensional CuO_2 plane. At a higher doping level, ruthenium doping induces a metal–insulator (MI) transition.

Figure 5 shows the temperature dependence of the resistivity for $La_{2-y}Sr_yCu_{0.99}Ru_{0.01}O_4$ between 4.2 and 300 K. As displayed in figure 5, with increase of the strontium content, the upturn of the resistivity at low temperature is suppressed and the temperature dependence becomes linear. The maximum T_c is obtained in the sample when the strontium content

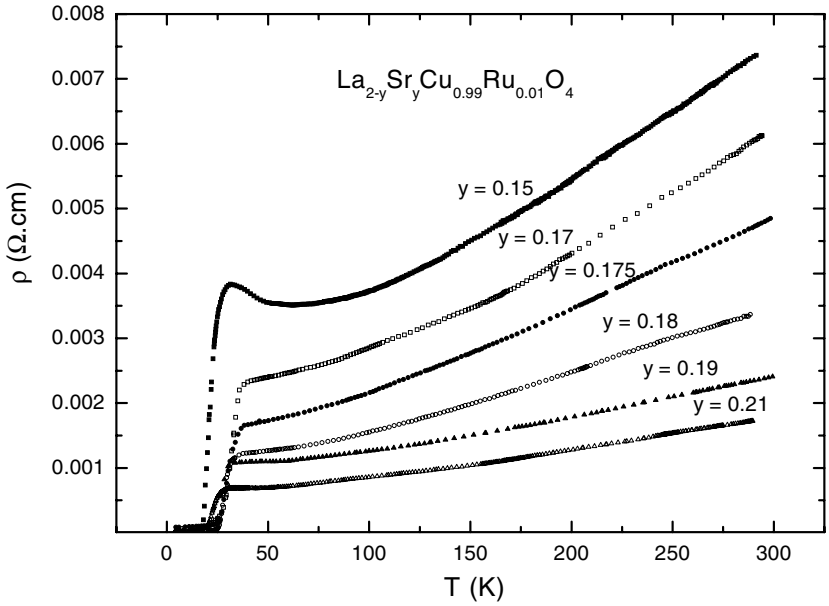

Figure 5. The temperature dependence of the resistivity for samples of $La_{2-y}Sr_yCu_{0.99}Ru_{0.01}O_4$.

$y = 0.17$. These phenomena can be explained by carrier concentration compensation. It is indicated that Ru doping reduces the number of holes and leads to a hole-filling effect due to doping with high-valence ions, while, the increase in strontium content provided carriers of holes, compensating for the decrease in the number of carriers which is caused by the doping with Ru.

Figure 6(a) shows the Sr content dependence of T_c for $La_{2-y}Sr_yCu_{1-x}Ru_xO_4$ ($x = 0.01$, 0.02, 0.03). In $La_{2-y}Sr_yCuO_4$, the sample is optimally doped with $y = 0.15$. As can be seen in figure 6(a), the strontium content where the maximum T_c is observed shifts to higher levels in the Ru-doped LSCO system, that is: $y = 0.17$ for $x = 0.01$; $y = 0.20$ for $x = 0.02$; and $y = 0.24$ for $x = 0.03$. These results indicate that Cu ions were replaced with Ru with higher ion valence, with a consequent reduction of the carrier concentration in the system. However, the reduced carrier concentration can be compensated by Sr doping. To test whether the rigid-band model holds or not in this case, we plotted renormalized $T_c/T_{c,max}$ versus the number of holes per Cu site, as shown in figure 6(b). It is well known that the formal oxidation states of Ru ions are between +4 and +5 [14]. The ion valence of Ru is considered to be 4.5, which is inferred from the XANES results [28]. In the LSCO system, the interstitial oxygen (δ) also contributes to the carrier concentration. However, δ can be considered to be approximately zero for $y \leqslant 2x + 0.4$ [28]. In figure 6(b), it is observed that the optimal T_c-peaks occur at approximately $x = 0.15$. A universal curve shows 'peaking' of T_c for the system doped with both Sr and Ru. This observed peak suggests that a rigid-band model holds for $La_{2-y}Sr_yCu_{1-x}Ru_xO_4$ ($x = 0.01$, 0.02, 0.03), and both Ru and Sr doping shift the chemical potential through strong features in the densities of states (DOSs). This indicates that T_c correlates with features in the DOS(E), such as a Van Hove singularity. Therefore, it is expected that the optimal T_c should occur for a given hole/Cu doping x as the Fermi level is tuned through a singularity.

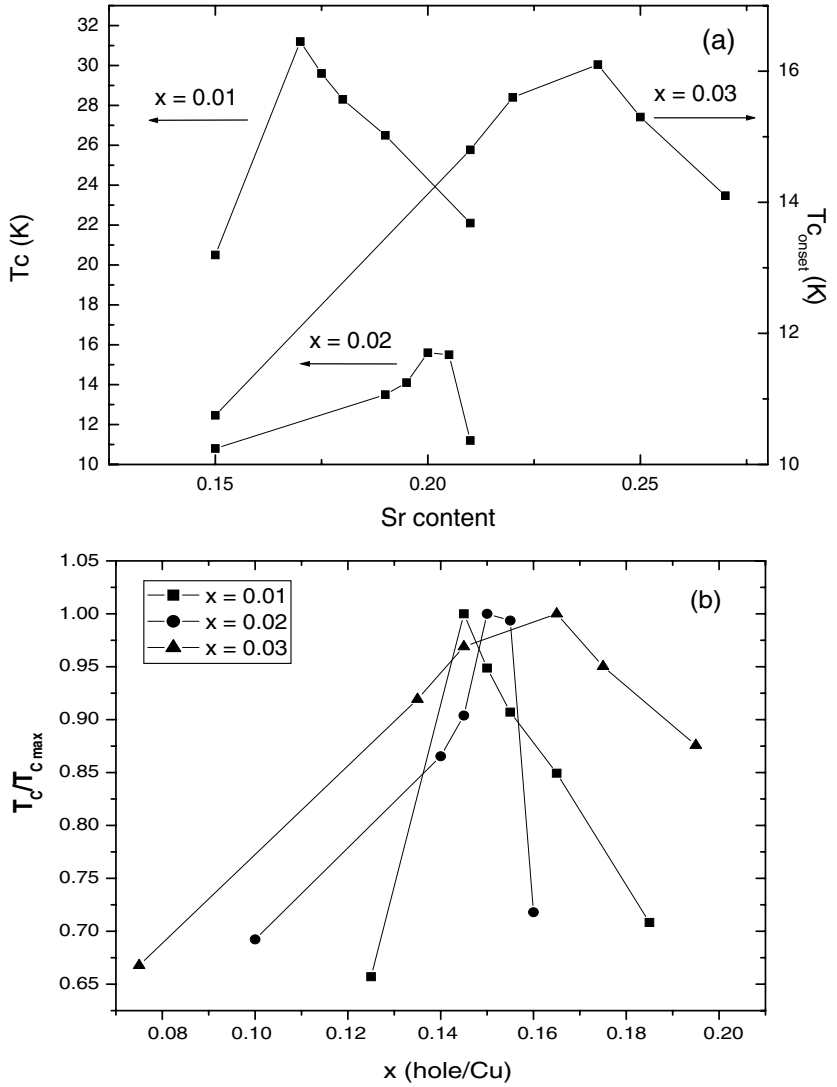

Figure 6. (a) The Sr content dependence of T_c for $La_{2-y}Sr_yCu_{1-x}Ru_xO_4$ ($x = 0.01$, 0.02, 0.03); (b) the renormalized T_c ($T_c/T_{c,max}$) as a function of the number of holes per Cu site for $La_{2-y}Sr_yCu_{1-x}Ru_xO_4$ ($x = 0.01$, 0.02, 0.03).

Table 1. T_c for $La_{1.85}Sr_{0.15}Cu_{1-x}Ru_xO_4$ ($T_{c(1)}$) and $La_{2-y}Sr_yCu_{1-x}Ru_xO_4$ ($T_{c(2)}$).

x	$T_{c(1)}$ (K)	$T_{c(2)}$ (K)
0.00	∼35	∼35
0.01	20.5	31.2 ($y = 0.17$)
0.02	10.8	15.6 ($y = 0.2$)
0.03 ($T_{c(onset)}$)	10.75	16.1 ($y = 0.24$)

In table 1, the dependences on the Ru content x of T_c for $La_{1.85}Sr_{0.15}Cu_{1-x}Ru_xO_4$ and $La_{2-y}Sr_yCu_{1-x}Ru_xO_4$ are shown. For $x = 0.03$, the resistance of the samples cannot decrease

to zero at 4.2 K; we use the onset temperature as the superconducting transition temperature. As can be seen in table 1, the strontium content corresponding to the maximum T_c shifts to a higher value: from 0.17 to 0.24 with increasing Ru doping. Superconductivity can be partly recovered by increasing the Sr content, but cannot recovered completely, especially for Ru doping at high levels. This suggests that Ru doping seems to have two effects on T_c: the first one is the decrease of the carrier concentration; and the second one is the effect of the Ru ion impurity doping into the Cu–O sheet. The decrease in T_c due to the first effect can be recovered by hole carrier compensation. With increase of x, the effect of the carrier concentration on the superconductivity becomes weak. Sr doping can almost recover the original T_c at $x = 0.01$. When $x \geqslant 0.02$, this cannot work. The effect of Ru ion doping on the superconductivity is dominated by the effect of chemical and magnetic disorder rather than the decrease of the carrier concentration. The decrease of T_c due to the destruction of the integrity of the superconducting CuO_2 plane caused by doping with Ru ions cannot be redeemed by hole carrier compensation. Doping of Ru at the Cu site introduces chemical disorder and a local magnetic moment into the CuO_2 plane. It destroys the periodic potential field and the antiferromagnetic interaction within the CuO_2 plane. Another pair-breaking mechanism that plays an important role in the suppression of the superconductivity occurs by spin-flip processes of scattering between the Cooper pairs and the magnetic atoms [34]. These processes are characterized by total spin conservation in the scattering event, so the spin of the Ru atom must flip when the Cooper pair is broken. So spin-flip scattering processes play a dominant role in the suppression of superconductivity in our case. The decreasing of T_c caused by the above factors cannot be redeemed by hole carrier compensation.

Ru doping of CuO_2 induces destruction of the integrity of the CuO_2 planes and the MI transition, as can be seen in figure 4. Similar behaviour of the hole localization has also been observed in Fe- and Ga-doped La214 systems [35]. It is known that the CuO_2 sheet of high-T_c superconductors is a conducting plane. The doping of impurity at the Cu site introduces disorder and a local magnetic moment into the CuO_2 plane. The observed MI transition in Ru-doped samples may originate from localization in CuO_2 planes induced by Ru ion doping. In figure 4, the superconductivity of the samples is suppressed when $x \geqslant 0.025$. The samples all show a MI transition when $x \geqslant 0.05$. The MI transition temperature increases with increase of x.

Figure 7 shows the $\rho(T)$ behaviour for samples of $La_{1.85}Sr_{0.15}Cu_{1-x}Ru_xO_4$ ($x = 0.05$ and 0.1). The inset shows the $T^{-1/3}$- and $T^{-1/4}$-dependences of $\ln \rho(T)$ below 100 K. The behaviour could be represented by a stretched power law T-dependence:

$$\rho(T) = \rho_0 \exp\{(T_0/T)^{\beta}\} \tag{2}$$

characteristic of a Mott variable-range hopping (VRH) mechanism [8]. Here, the value of β depends on both the dimension of the system and the behaviour of the DOS at the Fermi level. The value of β is predicted to be $1/4$ and $1/3$ for Mott 3D and 2D VRH conduction, respectively [36]. The presence of an interatomic Coulomb interaction, which depletes the DOS at the Fermi level, could lead to a Coulomb gap when the interaction is sufficiently strong [37]. This leads to the value $\beta = 1/2$. Moreover, β is known to change from $1/2$ to $1/4$ as the carrier concentration is increased [37–40], as has been documented from resistivity studies on the $Bi_2Sr_2Ca_{1-x}Y_xCu_2O_8$ system by Quitmann *et al* [40] We use equation (1) to fit the measured resistivity data, and find that for the $x = 0.05$ sample, data taken below 100 K are in better agreement with $\beta = 1/3$ than with $1/4$ or $1/2$. Comparison shows that the $x = 0.1$ sample is better fitted with $\beta = 1/4$. From these analyses, it is found that for the samples of $La_{1.85}Sr_{0.15}Cu_{1-x}Ru_xO_4$ with high doping levels the conducting mechanism changes from a 2D VRH mechanism to a 3D VRH mechanism.

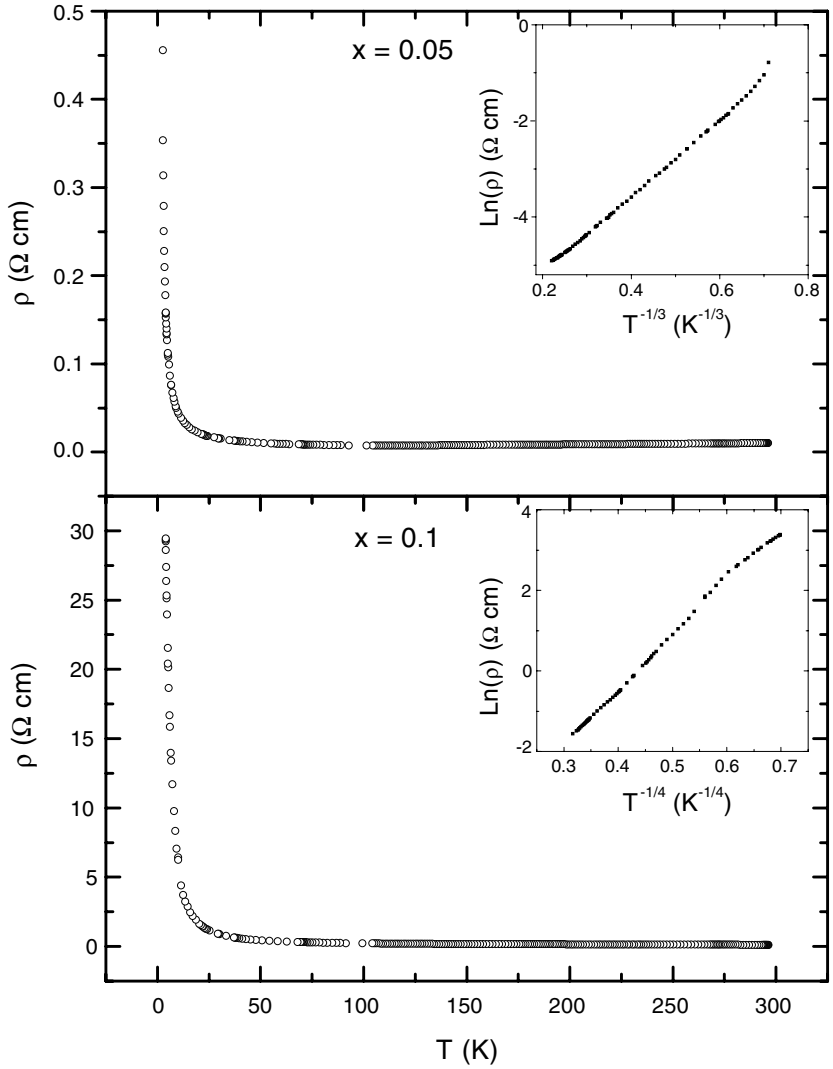

Figure 7. The $\rho(T)$ behaviour of samples of $La_{1.85}Sr_{0.15}Cu_{1-x}Ru_xO_4$ ($x = 0.05$ and 0.1). Inset: $T^{-1/3}$- and $T^{-1/4}$-dependences of $\ln \rho(T)$ below 100 K.

We can calculate an estimated value of the localization length (α^{-1}) from the T_0-values for samples of $La_{1.85}Sr_{0.15}Cu_{1-x}Ru_xO_4$ when $x = 0.05$. It can be obtained using the VRH relation [36, 42]

$$\alpha^{-1} \approx [k_B T_0 N(E_F)/16]^{-1/3} \tag{3}$$

where $N(E_F)$ is the DOS at the Fermi level and k_B is the Boltzmann constant. Using the measured values of the DOS reported for the $x = 0.05$ composition, which lie in the range 2–13 states eV^{-1}/cell [43, 44], and the T_0-values of 502 and 2447 K obtained for the $x = 0.05$ and 0.1 samples, respectively, we estimate localization length values α^{-1} in the range $3.1 < \alpha^{-1} < 5.7$ (lattice parameters) and $1.8 < \alpha^{-1} < 3.3$ (lattice parameters) for the $x = 0.05$ and 0.1 samples, respectively. The observed decrease in localization length (α^{-1}) with Ru substitution implies strong localization effects due to disorder.

4. Conclusions

The structure and transport properties of the Ru-doped LSCO system have been investigated by means of XRD and resistivity. The structure analysis implied that Cu ions are replaced by Ru ions. The effect of Ru doping has two components: one is hole carrier concentrations reducing due to the higher-valence ions; the other is the localization effect due to the Ru present as an impurity. Carrier concentration compensation via increasing Sr content leads to an increase of T_c. The rigid-band model holds for our system. It suggests that T_c correlates with the features of the DOS. For highly Ru-doped samples, the effect of the Ru doping on the superconductivity is dominated by disorder and destruction of CuO_2 plane integrity. The resistivity measurements show that Ru doping introduces a MI transition and this MI transition can be interpreted in terms of Anderson's two-dimensional localization. For the samples of $La_{1.85}Sr_{0.15}Cu_{1-x}Ru_xO_4$, when x changes from 0.05 to 0.1, the conducting mechanism changes from a 2D VRH mechanism to a 3D VRH mechanism.

Acknowledgments

This work was supported by the Natural Science Foundation of China and by the Ministry of Science and Technology of China (Grant No NKBRSF-G19990646).

References

[1] Bednorz J G and Müller K A 1986 *Physica* B **64** 189
[2] Ishikawa N, Kuroda N, Ikeda H and Yoshizak R 1992 *Physica* C **203** 284
[3] Kakinuma N, Ono Y and Koike Y 1999 *Phys. Rev.* B **59** 1491
[4] Naeini J G, Chen X K, Irwin J C, Okuya M, Kimura T and Kishio K 1999 *Phys. Rev.* B **59** 9642
[5] Mao Z, Xu G, Yan H, Wang B, Qiu X and Zhang Y 1998 *Phys. Rev.* B **58** 15116
[6] Wu X S, Jiang S S, Chen W M, Lin Z S, Jin X, Mao Z Q, Xu G J and Zhang Y H 1998 *Physica* C **294** 122
[7] Awana V P S, Agarwal S K, Das M P and Narlikar A V 1992 *J. Phys.: Condens. Matter* **4** 4971
[8] Sreedhar K, Metcalf P A and Honig J M 1994 *Physica* C **227** 160
[9] Wu X S, Mao Z Q, Lin J, Chen W M, Jin X, Xu G J, Zhang Y H, Pan F M and Jiang S S 1997 *Physica* C **282–287** 787
[10] Nakano T, Momona N, Matsuzaki T, Nagata T, Yokoyama M, Oda M and Ido M 1999 *Physica* C **317/318** 575
[11] Yang Li, Larrea J A, Baggio-Saitovitch J E, Che G C, Zhao Z X, Cao G H and Xu Z X 1999 *Physica* C **312** 283
[12] Koike Y, Takeuchi S, Hama Y, Sato H, Adachi T and Kato M 1997 *Physica* C **282–287** 1233
[13] Zhang Changjin, Zhang Jianwu and Zhang Yuheng 2000 *Physica* C **340** 168
[14] Ebbinghaus S, Hu Zhiwei and Reller A 2001 *J. Solid State Chem.* **156** 194
[15] Tsuei C C and Kirtley J R 2000 *Rev. Mod. Phys.* **72** 969
[16] Dai Pengcheng, Mook H A, Aeppli G, Hayden S M and Doan F 2000 *Nature* **406** 965
[17] Scalapino D J 1999 *Science* **284** 1282
[18] Xiao G, Cieplak M Z, Xiao J Q and Chien C L 1990 *Phys. Rev.* B **42** 8752
[19] Maeno Y, Hashimoto H, Yoshida K, Nishizaki S, Fujita T, Bednorz J G and Lichtenberg F 1994 *Nature* **372** 532
[20] Kuz'min E V, Ovchinnikov S G and Baklanov I O 2000 *Phys. Rev.* B **61** 15392
[21] Sigrist M, Agterberg D, Furusaki A, Honerkamp C, Ng K K, Rice T M and Zhitomirsky M E 1999 *Physica* C **317/318** 134
[22] Prafulla K J and Sankar P S 1999 *Physica* C **322** 110
[23] Yoshida Y *et al* 1999 *J. Phys. Soc. Japan* **68** 3041
[24] De Macro M, Graf D, Rijssenbeek J, Cava R J, Wang D Z, Tu Y, Ren Z F, Wang J H, Haka M, Toorongian S, Leone M J and Naughton M J 1999 *Phys. Rev.* B **60** 7570
[25] Rice T M and Sigrist H 1995 *J. Phys.: Condens. Matter* **7** L643
[26] Oguchi T 1995 *Phys. Rev.* B **51** 1385
[27] Mazin I I and Singh D J 1997 *Phys. Rev. Lett.* **79** 733
[28] Ebbinghaus S and Reller A 1997 *Solid State Ion.* **101–103** 1369

[29] Kamimura H, Koide S, Sekiyama H and Sugano S 1960 *J. Phys. Soc. Japan* **15** 1264
[30] Shannon R D 1976 *Acta Crystallogr.* A **32** 751
[31] Madelung E 1918 *Z. Phys.* 524
[32] Takagi H, Ido T, Ishibashi S, Uota M, Uchida S and Tokura Y 1989 *Phys. Rev.* B **40** 2254
[33] Braden M, Schweiss P, Heger G, Reichardt W, Fisk Z, Gamayunov K, Tanaka I and Kojima H 1994 *Physica* C **223** 396
[34] Vélez M, Cyrille M C, Kim S, Vicent J L and Schuller I K 1999 *Phys. Rev.* B **59** 14659
[35] Arai J, Ogawa S and Umezawa K 1993 *Physica* C **206** 257
[36] Mott N F and Davis E A 1979 *Electronic Processes in Non-Crystalline Materials* 2nd edn (Oxford: Clarendon)
[37] Efros A L 1976 *J. Phys. C: Solid State Phys.* **9** 2021
[38] Glukhov A M, Fogel N Ya and Shablo A A 1986 *Fiz. Tverd. Tela* **28** 1043
[39] Shafarman W N and Castner T G 1986 *Phys. Rev.* B **33** 3570
[40] Weng S L, Moehlecke S, Strongin M and Zangwill A 1983 *Phys. Rev. Lett.* **50** 1795
[41] Quitmann C, Andrich D, Jarchow C, Fleuster M, Beschoten B, Güntherodt G, Moshchalkov V V, Mante G and Manzke R 1992 *Phys. Rev.* B **46** 11813
[42] Ambegaokar V, Halperin B I and Langer J S 1972 *Phys. Rev.* B **4** 2612
[43] Greene R L, Maletta H, Plaskett T S, Bednorz J G and Müller K A 1987 *Solid State Commun.* **63** 379
[44] Uchida S, Takagi H, Kishio K, Kitazawa K, Fueki K and Tanaka S 1987 *Japan. J. Appl. Phys.* **26** L443